

International Journal of Modern Physics E  
© World Scientific Publishing Company

## Overview of event-by-event analysis of high energy nuclear collisions

Tapan K. Nayak

*CERN CH-1211, Geneva 23, Switzerland  
and*

*Variable Energy Cyclotron Centre, Kolkata-700064, India  
Tapan.Nayak@cern.ch*

Received (received date)

Revised (revised date)

The event-by-event analysis of high energy nuclear collisions aims at revealing the richness of the underlying event structures and provide unique measures of dynamical fluctuations associated with QGP phase transition. The major challenge in these studies is to separate the dynamical fluctuations from the many other sources which contribute to the measured values. We present the fluctuations in terms of event multiplicity, mean transverse momentum, elliptic flow, source sizes, particle ratios and net charge distributions. In addition, we discuss the effect of long range correlations, disoriented chiral condensates and presence of jets. A brief review of various probes used for fluctuation studies and available experimental results are presented.

### 1. Introduction

The event-by-event analysis of high energy nuclear collisions aims at searching for dynamical fluctuations associated with the phase transition of normal nuclear matter to the Quark-Gluon Plasma (QGP). Fluctuations of thermodynamic quantities provide an unique framework for studying the nature of QGP phase transition and provide direct insight into the properties of the system created in high energy heavy-ion collisions<sup>1,2,3</sup>. Large fluctuations in energy density due to droplet formation<sup>4</sup> are expected if the phase transition is of first order. A second order phase transition may lead to divergence in specific heat and increase in fluctuations of energy density due to long range correlations in the system. Furthermore, the prospect of locating the critical point of the QGP phase transition, where the fluctuations are predicted to be largely enhanced<sup>5</sup>, makes this study rather interesting and challenging. The rapid development in the event-by-event study in recent years is related to the availability of high beam energies and sophisticated experiments with large acceptance detectors. The regime of event-by-event study spans from understanding the bulk properties of matter to high  $p_T$  particles including jets.

The challenge of event-by-event studies is that, beyond the fluctuations linked to the details of the phase transition, there are a number of other fluctuations which appear. There are numerous well-established physical sources of event-by-

2 *Tapan K. Nayak*

event fluctuations in high-energy nucleus–nucleus collisions, *viz.*, geometrical (impact parameter, number of participants, detector acceptance), energy, momentum, temperature, charge conservations, anisotropic flow, Bose-Einstein correlations, resonance and string decays, jets and minijets and effect of quantum statistics. Many exotic phenomena may also occur and significantly impact the observed fluctuations. Among them are formation of Disoriented Chiral Condensates (DCC), colour collective phenomena and formation of colour ropes.

Fluctuations in physical quantities can shed light on the nature of the matter created in relativistic heavy-ion collisions. Recently there has been a debate over whether the bulk of the matter created at RHIC behaves like a perfect fluid<sup>6</sup>. Fluctuation in elliptic flow might provide a sensitive probe towards answering this question. Fluctuations of conserved quantities like net electric charge, baryon number and strangeness are predicted to be significantly reduced in a QGP scenario as they are generated in the early plasma stage of the system created in heavy-ion collisions with quark and gluon degrees of freedom. It has been suggested that the processes following QGP hadronization like hadronic rescattering and resonance decays may almost completely wipe out fluctuations originally developed in the QGP phase. Thus the propagation of fluctuation from initial stages of collision to the freeze-out has to be considered before making any conclusions about the fluctuations from QGP and non-QGP stages<sup>7</sup>.

The information content of the amount of fluctuation is inherent in the variance of the width of the distribution of a given observable, expressed in terms of

$$\omega_X = \frac{\sigma_X^2}{\langle X \rangle}, \quad (1)$$

where  $X$  is the variable under study,  $\sigma_X^2$  is the variance of the distribution and  $\langle X \rangle$  denotes the mean value. The task is to distinguish between statistical fluctuations and those which have dynamical origin. Several methods have been put forward suggesting ways to infer about the presence of dynamical fluctuations. In order to infer about the presence of non-statistical fluctuations, one needs to compare the experimental results with known models which incorporate all the known phenomena. An alternate or may be complimentary procedure to probe the fluctuations in a model independent manner would be to compare experimental distributions of real data to those of the mixed events. In this manuscript, we discuss various probes of fluctuations and recent experimental findings.

## 2. Volume fluctuations and centrality selection

The volume fluctuation<sup>1</sup> arises through the measurement of multiplicity,  $N$ ,

$$N = \rho V, \quad (2)$$

where  $\rho$  is the density and  $V$  is the volume. The fluctuation in  $N$  is expressed as:

$$\langle \delta N^2 \rangle = \langle \delta \rho^2 \rangle \langle V \rangle^2 + \langle \rho \rangle^2 \langle \delta V \rangle^2. \quad (3)$$

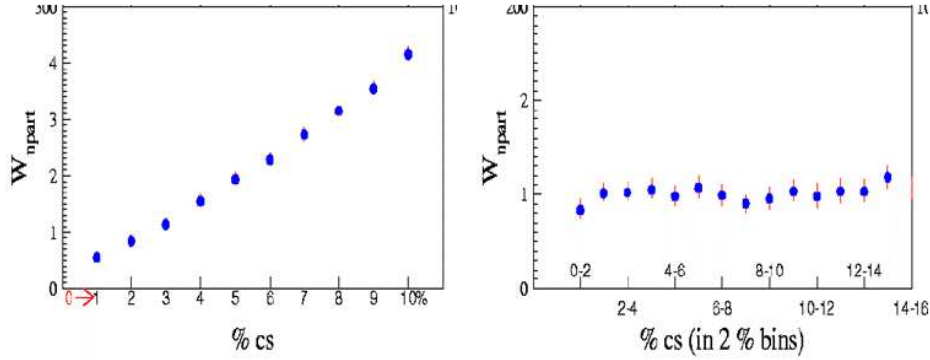


Fig. 1. The fluctuation in the number of participants ( $\omega_{npart}$ ) as a function of centrality, expressed as a percentage of cross section for Pb-Pb collisions at  $\sqrt{s_{NN}}=17.3$  GeV. The increase of centrality bin from very narrowly defined (0-1%) to wider ones (0-10%) (shown in the left panel) causes an increase in the fluctuation. The right panel shows that for narrow centrality bins the fluctuations remain minimal and close to unity.

Since the main interest is on the fluctuation of the density,  $\langle \rho \rangle^2$ , the second term containing  $\langle \delta V \rangle^2$  has to be estimated in order to make any conclusion. One of the ways to control the volume fluctuation is by making proper centrality selection.

In case of heavy-ion collisions, centrality is characterized by the impact parameter,  $b$ , of the collision, which also can be expressed in terms of the number of participating nucleons,  $N_{part}$ . A given centrality class has a set of values of  $b$  or  $N_{part}$ . As there is no real control over the impact parameter of the collision in heavy-ion experiments, geometric fluctuation is unavoidable in the fluctuation of any extensive quantities<sup>1,8</sup>. The importance of centrality selection for fluctuation studies can be understood in terms of a participant model<sup>2,8,9</sup>. Since it is not possible to measure either  $b$  or  $N_{part}$  directly, estimations of these quantities are based on calorimetric and multiplicity measurements. For events in a given centrality class,  $b$  or  $N_{part}$  values are extracted in a model dependent way. The number of produced particles ( $N$ ) in a collision depends on the centrality of the collision expressed in terms of  $N_{part}$  and the number of collisions suffered by each particle:

$$N = \sum_{i=1}^{N_{part}} n_i, \quad (4)$$

where  $n_i$  is the number of particles produced in the detector acceptance by the  $i^{th}$  participant. The mean value of  $n_i$  is the ratio of the average multiplicity in the detector coverage to the average number of participants, i.e.,  $\langle n \rangle = \langle N \rangle / \langle N_{part} \rangle$ . The fluctuation in particle multiplicity has a main contribution from the fluctuations in  $(N_{part})$ . In order to infer any dynamical fluctuation arising from various physics processes one has to make sure that the fluctuations in  $N_{part}$  are minimal.

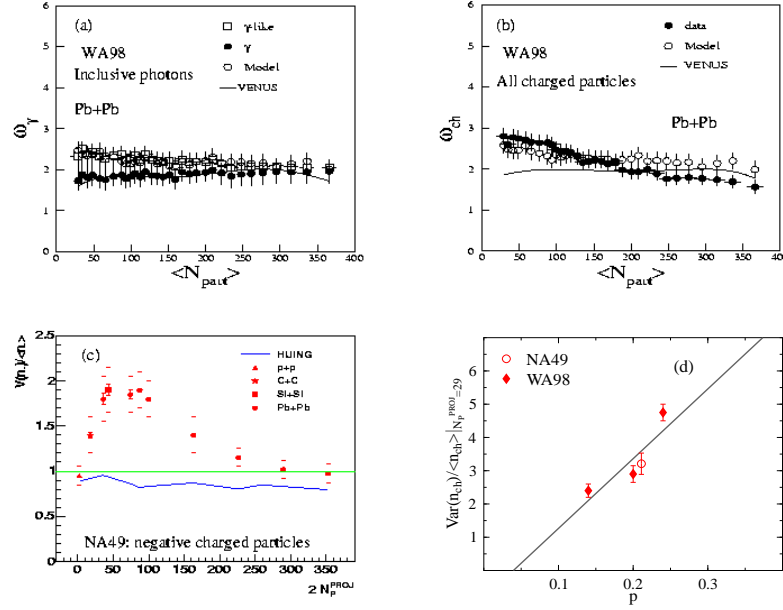
4 *Tapan K. Nayak*

Fig. 2. Multiplicity fluctuations at the SPS energies for (a) photons and (b) charged particles from the WA98 experiment at the SPS, (c) charged particles from the NA49 experiment at the SPS and (d) comparison of the scaled variance of charged particles for semi-central collisions as a function of acceptance for the WA98 and NA49 setup.

Fluctuations in  $N_{part}$  have been studied at the SPS by the WA98 experiment<sup>8</sup> where the centrality selections were made by using the mid-rapidity and the zero-degree calorimeters.  $N_{part}$  values are calculated using the VENUS event generator<sup>10</sup> and the WA98 simulation framework. Figure 1 shows fluctuations in  $N_{part}$  for various ranges of centrality bins expressed in terms of percentage of cross section. Fluctuation seems to increase for broad centrality class as shown in the left panel of the figure, whereas the fluctuations for narrow centrality bins (such as 0–2%, 2–4%, 4–6%, ..., 50–52%) remain around unity for most of the centrality bins. This suggests narrow cross section slices in the centrality bins are preferable for fluctuation studies.

### 3. Multiplicity fluctuations

Depending on the nature of QGP phase transition, there will be large density fluctuations leading to droplet formation and hot spots<sup>4</sup>. These will give rise to large rapidity and multiplicity fluctuations of produced particles and have distinct effects on the space time extent of the source. Multiplicity of produced particles characterizes the evolving system in a heavy-ion collision and thus fluctuation in multiplicity may provide a distinct signal of the QGP phase transition<sup>2,8</sup>.

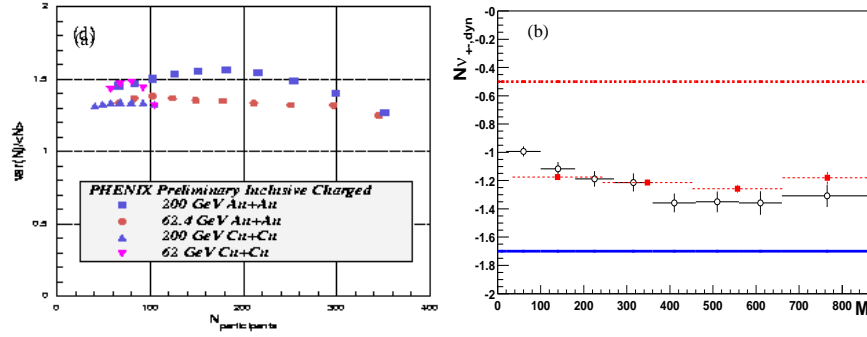


Fig. 3. Multiplicity fluctuations of charged particles at the RHIC energies for PHENIX experiment (left panel) and STAR experiment (right panel).

Since multiplicity distributions for narrow centrality bins can be described by Gaussian distributions, their fluctuations are expressed in terms of scaled variance, defined as,  $\omega = \text{var}(N)/\langle N \rangle$ , where  $\langle N \rangle$  and  $\text{var}(N)$  represent the variance and mean of the multiplicity distribution, respectively. Figure 2 shows observed scaled variance for SPS and RHIC energies. The results from the WA98 experiment<sup>8</sup>, those corresponding to photons and charged particles, are compared to different model calculations. Although the experimental data is consistent with the model calculations within the quoted error bars, the increasing trend of fluctuation for charged particles towards peripheral collisions is clearly visible. The scaled variance of charged particles as a function of centrality as measured by NA49 experiment<sup>11</sup> shows a non-monotonic behaviour, especially at mid central regions. A good comparison has been made between the results of the charged particles for WA98 and NA49 experiments by taking the acceptance and fraction ( $p$ ) of registered particles into account. As shown in Figure 2(d), the results of both the experiments are in good agreement. The PHENIX data<sup>12,13</sup> for multiplicity fluctuations are shown in the left panel of Figure 3 for Au–Au and Cu–Cu collisions at RHIC energies. The Cu–Cu data at  $\sqrt{s_{\text{NN}}} = 62.4$  GeV shows a small structure for non-central collisions whereas at higher energies the data are smoother. Dynamical fluctuations, expressed in terms of  $N\nu_{+-\text{dyn}}$  are shown in the right panel of Figure 3 as function of collision centrality for Au–Au collisions at  $\sqrt{s_{\text{NN}}} = 130$  GeV as measured by the STAR experiment<sup>14</sup>. The open circles show the measured data compared to the charge conservation limit (dotted line), resonance gas (solid line) and HIJING calculations (solid squares). Detailed understanding of these results would require considerations of centrality selection and detector effects.

#### 4. Temperature and $\langle p_{\text{T}} \rangle$ Fluctuations

The  $\langle p_{\text{T}} \rangle$  of emitted particles in an event is related to the temperature of the system. Thus the event-by-event fluctuations of average  $p_{\text{T}}$  is sensitive to the temperature

6 *Tapan K. Nayak*

fluctuations predicted for the QGP phase transition. Several measures of fluctuation have been introduced in order to probe the dynamical fluctuation from the measured values, some of these include<sup>15</sup>:

$$F_{p_T} = \frac{\Omega_{data} - \Omega_{baseline}}{\Omega_{baseline}}, \quad (5)$$

$$\text{where } \Omega = \sigma_{M_{p_T}} / \langle N \rangle, \quad (6)$$

$$\Delta\sigma_{p_T}^2 \equiv \frac{1}{\varepsilon} \sum_{j=1}^{\varepsilon} N_j (\langle p_T \rangle_j - \overline{p_T})^2 - \sigma_{\hat{p}_T}^2 \equiv 2\sigma_{\hat{p}_T} \Delta\sigma_{p_T}, \quad (7)$$

$$\Phi_{p_T} \equiv \left[ \frac{1}{\varepsilon} \sum_{j=1}^{\varepsilon} \frac{N_j^2}{\langle N \rangle} (\langle p_T \rangle_j - \overline{p_T})^2 \right]^{1/2} - \sigma_{\hat{p}_T}. \quad (8)$$

$$\sigma_{\langle p_T \rangle, \text{dynamical}}^2 \equiv \frac{1}{\varepsilon} \sum_{j=1}^{\varepsilon} \frac{1}{N_j(N_j - 1)} \sum_{i \neq i'=1}^{N_j} \delta p_{T_{ji}} \delta p_{T_{ji'}}, \quad (9)$$

where  $\varepsilon$  is the number of events,  $j$  is the event index,  $N_j$  is the event multiplicity,  $\langle N \rangle$  is the mean multiplicity,  $i$  is a particle index, and  $\delta p_{T_{ji}} = p_{T_{ji}} - \overline{p_T}$ . For minimal variations of  $N_j$  within the event ensemble, one can define:

$$\Delta\sigma_{p_T} \cong \Phi_{p_T} \cong \frac{\langle N \rangle - 1}{2\sigma_{\hat{p}_T}} \sigma_{\langle p_T \rangle, \text{dynamical}}^2 \quad (10)$$

$$\text{and } \langle \Delta p_{i,1} \Delta p_{i,2} \rangle = \frac{1}{N_{\text{event}}} \sum_{k=1}^{N_{\text{event}}} \sum_{j=1, i \neq j}^{N_k} \frac{\delta p_{T,j} \delta p_{T,i}}{N_k(N_k - 1)} \quad (11)$$

Figure 4 shows the centrality dependence of dynamical fluctuations reported by CERES<sup>16</sup>, NA49<sup>17</sup>, PHENIX<sup>18</sup> and STAR<sup>19</sup> experiments. The results presented in Figure 4(d) show a smooth variation of fluctuation with centrality whereas the other measurements show non-monotonic behaviour. Efforts are being made to understand the nature and origin of these fluctuations. Because of the choice of several variables, extraction of an excitation energy plot combining data from SPS to RHIC is not straightforward. It is of interest to us to have a common framework for presenting the results from different experiments.

In order to be more sensitive to the origin of fluctuations, differential measures have been adopted where the analysis is performed at different scales (varying bins in  $\eta$  and  $\phi$ ). The scale dependence of  $\langle p_T \rangle$  fluctuation for three centralities in Au–Au collisions at  $\sqrt{s_{\text{NN}}} = 200$  GeV<sup>20</sup> is shown in Figure 5. The extracted autocorrelations are seen to vary rapidly with collision centrality, suggesting that fragmentation is strongly modified by a dissipative medium in more central collisions relative to peripheral collisions. Further studies for different charge combinations will provide more detailed information.

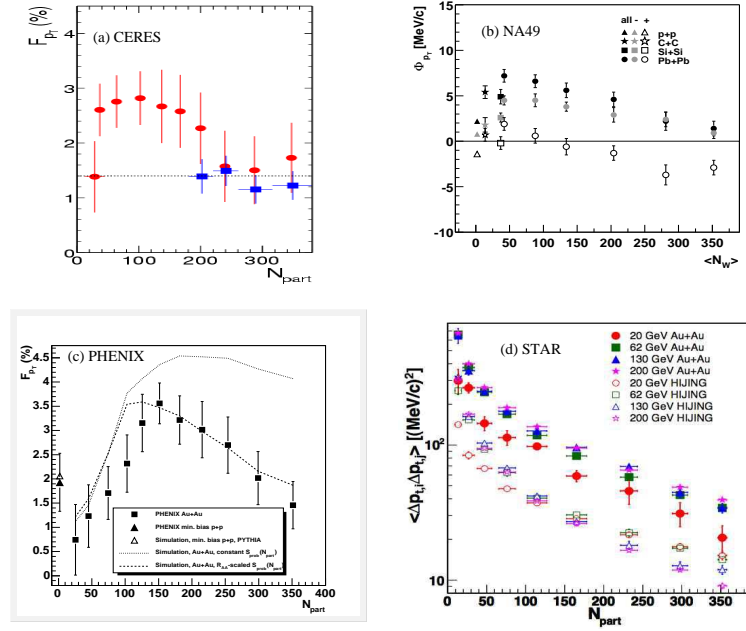


Fig. 4. Dynamical  $\langle p_T \rangle$  fluctuations as a function of centrality of the collision from (a) CERES, (b) NA49, (c) PHENIX and (d) STAR experiments.

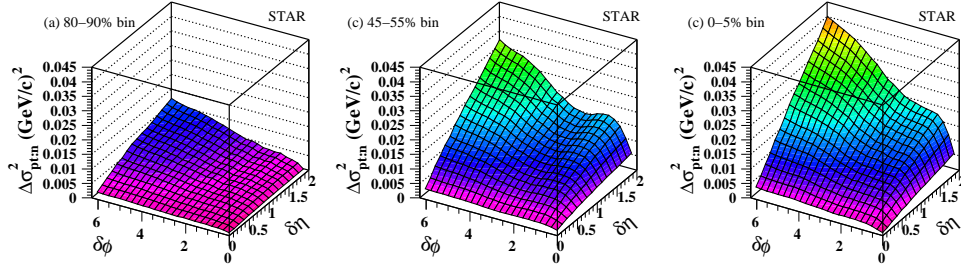


Fig. 5. Scale dependence of  $\langle p_T \rangle$  fluctuation within the STAR acceptance expressed in terms of per-particle variance difference.

## 5. Fluctuations in elliptic flow and eccentricity

Fluctuations in physical quantities can discern whether the matter created in heavy-ion collisions is a perfect fluid or not. A dissipation in a non-perfect fluid is related to the fluctuations of the physical quantities<sup>21,22</sup>. Fluctuation in elliptic flow ( $v_2$ ) has been proposed to be a sensitive probe for this study, as it might reflect the fluctuation in the initial spatial eccentricity. Fluctuation in  $v_2$  is argued to be also sensitive to the following physical effects: (a) filamentation instability initiated due to the strong momentum anisotropy of the partonic system, and the generation and

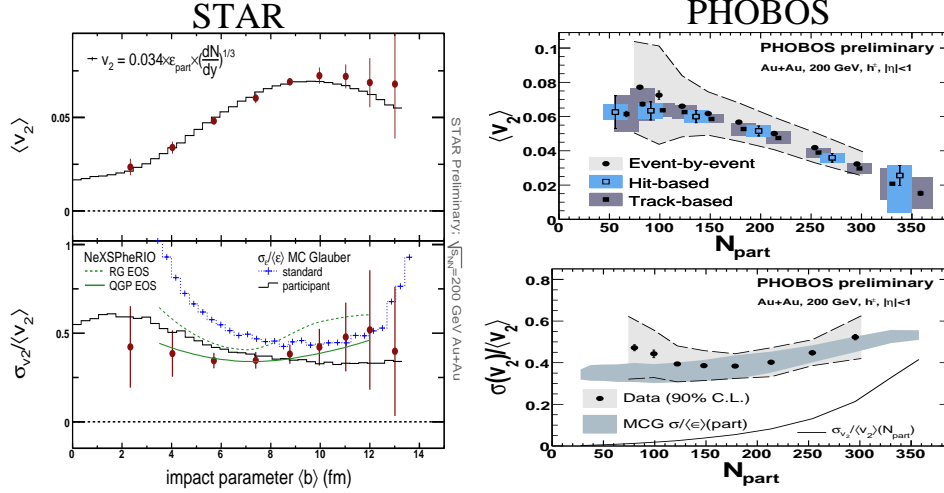
8 *Tapan K. Nayak*

Fig. 6. The mean of the  $v_2$  distribution ( $\langle v_2 \rangle$ ) (top panels) and the r.m.s. width of the the distribution ( $\sigma_{v_2}$ ) scaled by the mean (bottom panels) for Au–Au collisions at  $\sqrt{s_{NN}} = 200$  GeV as measured by for STAR and PHOBOS collaborations.

subsequent explosions of the topological clusters and (b) multiplicity fluctuations. Thus, study elliptic flow ( $v_2$ ) on an event-by-event basis is expected to provide sensitivity to initial conditions for the matter created in heavy-ion collisions.

Recently both STAR and PHOBOS experiments have studied the fluctuations in elliptic flow in Au–Au collisions at  $\sqrt{s_{NN}} = 200$  GeV. The results are presented in Figure 6. The left panel shows the STAR results<sup>23</sup> for mean ( $\langle v_2 \rangle$ ) and relative fluctuations ( $\sigma_{v_2}/\langle v_2 \rangle$ ) as a function of the impact parameter, whereas the right panel shows the PHOBOS results<sup>24</sup> for the same quantities as a function of the number of participants. The relative fluctuations have been found to be about 36-40%. The interesting fact is that these values can be nicely reproduced by Monte-Carlo Glauber calculations of participant eccentricity, implying that the later collision stages do not significantly alter the fluctuation pattern. These results, along with results for other colliding systems and collision energies, will be able to constrain the inputs to hydrodynamic model calculations.

## 6. Event-by-event analysis of HBT radii

The information about the space-time structure of the emitting source can be extracted by the method of intensity interferometry techniques, known as Hanbury-Brown Twiss (HBT) correlations. Due to lack of statistics, the analysis of HBT correlations are performed over a large number of events. But in reality, the space-time structure of the emitting source may vary from one event to other. This is illustrated in Figure 7, where the energy density distribution is plotted in  $x - y$



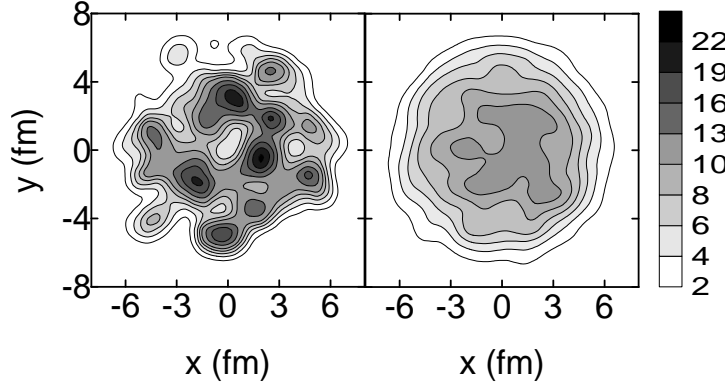


Fig. 7. Energy density distributions (in units of  $\text{GeV}/\text{fm}^3$ ) plotted in  $x - y$  source dimensions for a single event (left panel) and average over 30 events.

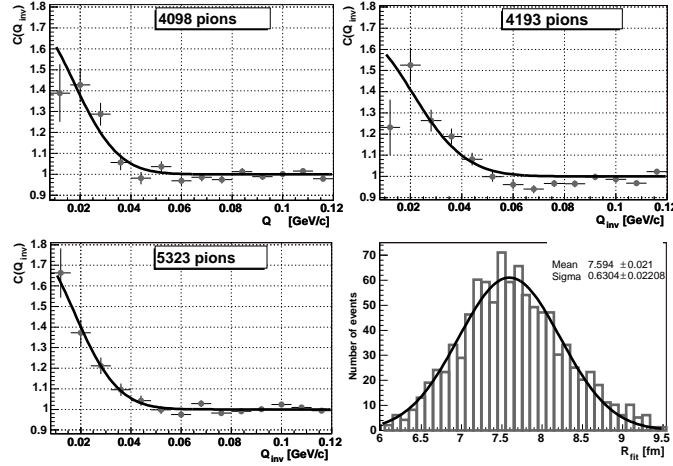


Fig. 8. Single event correlation functions for three events with different number of reconstructed pions. The bottom right panel shows the distribution of reconstructed radii

source dimensions<sup>25</sup>. The distribution for a typical single event (left panel) shows several blobs of high density matter, whereas the distribution is smoothed out if an average is taken (right panel). It would be interesting to perform correlation function analysis for single events from which one can understand fluctuations in three dimensional source sizes. These fluctuations will provide important information about the initial source sizes and could be related to initial eccentricity as well.

An attempt has been made to perform single event HBT analysis for the simulated events corresponding Pb-Pb collisions at  $\sqrt{s_{\text{NN}}} = 5500$  GeV in the framework

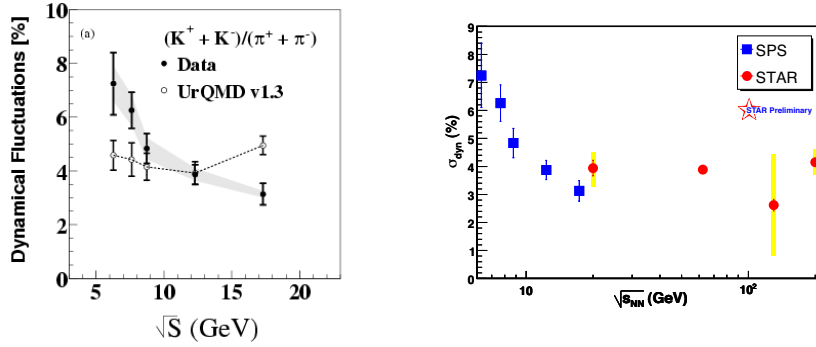
10 *Tapan K. Nayak*

Fig. 9. Excitation function for  $\sigma_{dyn}$  of  $[K^+ + K^-]/[\pi^+ + \pi^-]$  ratio at the SPS (left panel) and with an extension to RHIC (right panel).

of ALICE experiment<sup>26</sup> at the LHC. Figure 8 shows the HBT correlations for three typical events and a distribution of the reconstructed radii taken over several events. The results indicate that it will be possible study single-event interferometry in ALICE which may for the first time be sensitive enough to source fluctuations.

## 7. Fluctuation in particle ratio

Relative production of different particle species produced in the hot and dense matter might get affected when the system goes through a phase transition. Of particular interest is the strangeness fluctuation in terms of the ratio of kaons to pions. Large broadening in the yields of kaons to pions has long been predicted because of the differences in free enthalpy of the hadronic and QGP phase. This could be probed through the fluctuation in the  $K/\pi$  ratio.

A detailed study at SPS has been carried out at several beam energies<sup>27</sup>. The ratio of inclusive mid-rapidity yields of  $\langle K^- \rangle / \langle \pi^- \rangle$  has an increasing trend with beam energy, whereas a horn structure is seen in the ratio of  $\langle K^+ \rangle / \langle \pi^+ \rangle$ . It has been shown that the dynamical fluctuations ( $\sigma_{dyn}$ ) in the ratio of  $p/\pi$  has an increasing trend with respect to beam energy. This feature could be explained by model calculations. At the same time  $\sigma_{dyn}$  in the  $K/\pi$  ratio is seen to decrease with beam energy, a behavior which could not be explained by the same model. The  $\sigma_{dyn}$  values at SPS energies are shown in the left panel of Figure 9. The STAR experiment has performed a similar study on the event-wise fluctuations of the  $K/\pi$  ratio for Au–Au collisions at  $\sqrt{s_{NN}} = 62.4$  GeV and  $\sqrt{s_{NN}} = 200$  GeV<sup>28</sup>. A reduction as a function of centrality is reported for the two energies. The right panel of Figure 9 shows an excitation energy plot for  $K/\pi$  ratio extended up to the highest RHIC energies. The fluctuation decreases with increasing energy up to the highest SPS energy and remains constant at higher RHIC energies. Theoretical investigations<sup>29,30</sup> are underway to explain such behaviour.

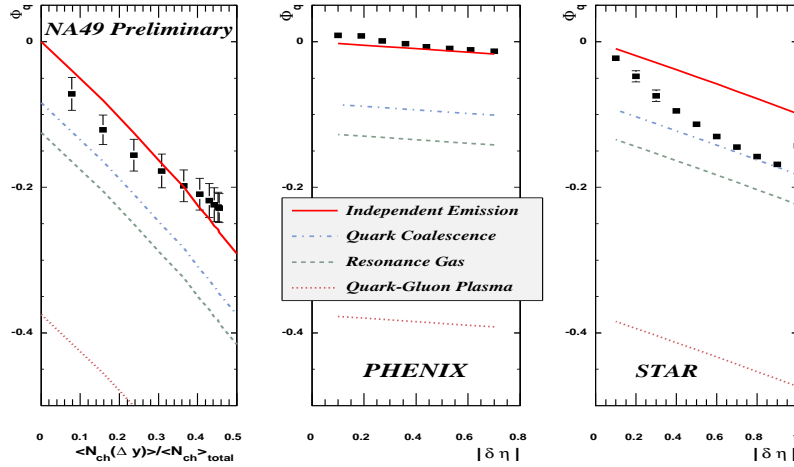


Fig. 10. Dynamical fluctuation of net charge for NA49, PHENIX and STAR experiments.

## 8. Net charge fluctuations

Fluctuations of conserved quantities like electric charge, baryon number or strangeness are predicted to be significantly reduced in a QGP scenario as they are generated in the early plasma stage of the system created in heavy-ion collisions with quark and gluon degrees of freedom<sup>31,32</sup>. The fluctuation generated at the QGP stage will increase as the system evolves in time<sup>7,33</sup>. Net charge fluctuations have been measured by experiments at SPS and RHIC using different fluctuation measures. Among these are  $\Phi_q$  of NA49<sup>34</sup>,  $\nu_{+-,dyn}$  of STAR<sup>14</sup> and  $v(Q)$  as well as  $\nu_{+-,dyn}$  used by PHENIX<sup>35</sup>. A common framework which relates these variables has been used to compile the available results<sup>36,37</sup>. The results from these experiments are shown in Figure 10, along with predictions from independent particle emission, quark coalescence, resonance gas and a QGP scenario. Both NA49 and PHENIX results are consistent with the independent particle emission scenario, whereas the result for STAR is close to the case of the quark coalescence model.

## 9. Higher Moments of net charge

Recently, lattice computations<sup>38,39,40</sup> have been performed to study hadronic fluctuations. In the lattice framework one calculates the susceptibilities which are variances and covariances of various quantum numbers. These susceptibilities provide valuable information on the degrees of freedom in the hot phase of QCD. The non-linear susceptibilities (NLS) have been calculated which are higher derivatives of the pressure with respect to the chemical potential. These calculations predict an enhancement of fluctuation in the hadronic phase and suppression of fluctuations

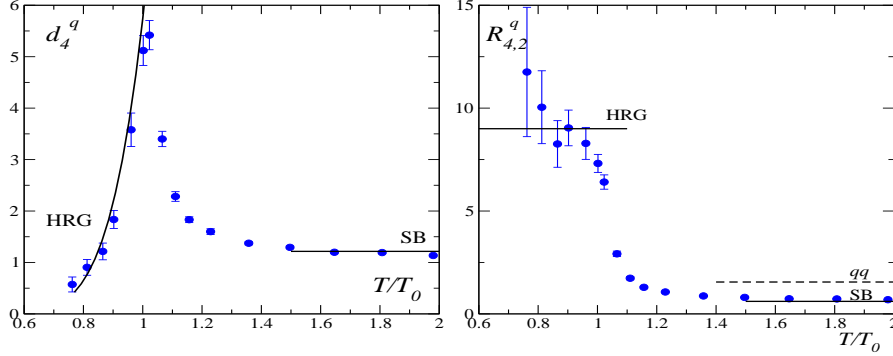
12 *Tapan K. Nayak*

Fig. 11. The fourth-order cumulant moments of net charge from the lattice calculations (left panel). The lines for  $T/T_0 < 1$  are the hadron resonance gas model results. The right panel shows the ratio of fourth to second order cumulants of quark number at  $u = 0$ .

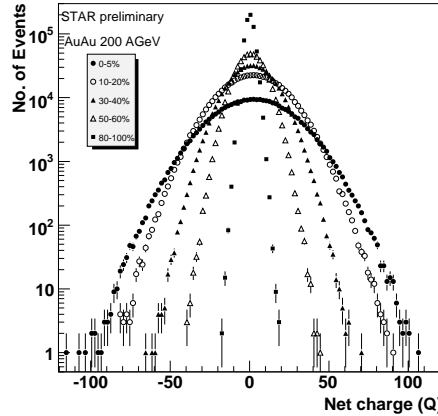


Fig. 12. Net charge distributions of particles with  $p_t$  below 1 GeV/c for Au–Au collisions at  $\sqrt{s_{NN}} = 200$  GeV at different centralities.

in the high temperature phase of the QGP. A prominent structure in the higher order moments of net charge distributions have been observed for temperatures close to the transition temperature. Figure 9 shows the 4th order cumulants of the net charge and the ratio of the second to the fourth order cumulants of the net charge distributions<sup>40</sup>. In the hadronic phase this ratio has an increase with increasing temperature up to the critical temperature,  $T_C$ , and a rapid suppression is seen in the high temperature phase of QGP.

While the origin of this structure is under discussion by various authors, it provides an excellent opportunity for experiments to make a study. Figure 12 shows the net charge distributions of particles with  $p_T$  below 1 GeV/c for Au–Au collisions at  $\sqrt{s_{NN}} = 200$  GeV for different centralities in the STAR experiment within a pseudorapidity coverage of  $-1 \leq \eta \leq 1$ . Efforts are underway to study higher order moments of these distributions by making smaller bins in detector acceptances and

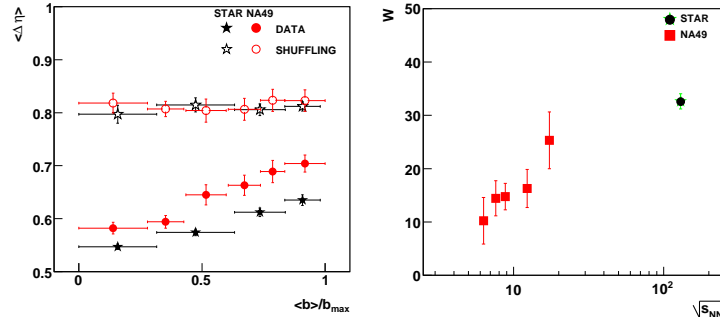


Fig. 13. (a) The width of the balance function as a function of centrality for experimental data along with results for shuffled bins (b) Normalized parameter ( $W$ ) of balance function as a function of beam energy.

$p_T$ . The ratio of the second to fourth order moments, can be expressed in terms of the kurtosis of the net charge distributions. This can provide a measure of the deviation from a normal distribution in terms of its peakiness (positive kurtosis) or flatness (negative kurtosis) at the mean. Detailed studies are being performed.

## 10. Balance functions

The method of Balance Functions (BF)<sup>41</sup>, provides a measure of correlation of oppositely charged particles produced in heavy-ion collisions. The basic idea is that the charged hadrons are produced locally as oppositely charged-particle pairs. The particles of such a pair are separated in rapidity due to the initial momentum difference and secondary interaction with other particles. The particles of a pair produced earlier are separated further in rapidity compared to the particles coming from a pair produced later in time. Since the width of the correlation can be related to the time of hadronization of the charged particles, this would signal any possible delayed hadronization, corresponding to QGP formation.

The BF can be studied as a function of several parameters in order to gain insight about different physics mechanisms. One of the basic studies may be performed in terms of the relative pseudorapidity difference for all charged-particles. In addition, there is the possibility to study the BF for different particle species which could give insight to the different mechanisms that are important in the creation process for the species. Furthermore the BF can be studied as a function of the azimuthal angle<sup>42</sup>,  $\phi$ , and thus translate the correlation function into a measure of transverse flow. By doing that one will be able to quantify the transverse flow for different particle species. The study of BF as a function of the invariant relative momentum  $Q_{inv}$  might yield a clear insight for interpreting the physics of the balancing charges.

Both STAR<sup>43</sup> and NA49<sup>44</sup> experiments have made detailed measurements of the BFs for various colliding systems, centralities, pseudorapidity intervals as well

as for identified charged particles. Here we present two of these studies; centrality dependence and excitation energy dependence of BF widths. The left panel of Figure 13 shows the width of the BFs as function of the normalized impact parameter for Pb–Pb collisions at  $\sqrt{s_{\text{NN}}}=17.2$  GeV and Au–Au collisions at  $\sqrt{s_{\text{NN}}}=130$  GeV. The widths of the BF decrease from peripheral to central collisions in experimental data whereas the shuffled data shows no such reduction. The decrease in the width can be quantified by the use of a normalized parameter,  $W$ , expressed as enhancement in the width in the data with respect to the corresponding shuffled values. The values of  $W$  are plotted in the right panel of Figure 13 as a function of beam energy<sup>45</sup>. The increase of the  $W$  from SPS to RHIC may be interpreted in terms of a delayed hadron scenario.

## 11. Short and Long range correlations

A copious production of partons, mainly gluons, due to hard and semi-hard processes, is expected in heavy-ion collisions. During the early stages of collision the system is on average locally colourless, but random fluctuations can break the neutrality<sup>46</sup>. Since the system is initially far from equilibrium, specific colour fluctuations can exponentially grow in time and then noticeably influence the evolution of the system. Additional valuable information on the collision dynamics, specifically on the string fusion and percolation phenomenon, may be obtained in the event-by-event studies of the correlations between various observables measured in separated rapidity intervals (long range correlations). These can be studied in different rapidity intervals for multiplicity correlations,  $\langle p_{\text{T}} \rangle$  correlations and multiplicity- $\langle p_{\text{T}} \rangle$  correlations. Model-independent detailed experimental information on long-range correlations between such observables as charge, strangeness, multiplicity and  $\langle p_{\text{T}} \rangle$  could be a powerful tool to discriminate theoretical reaction mechanisms.

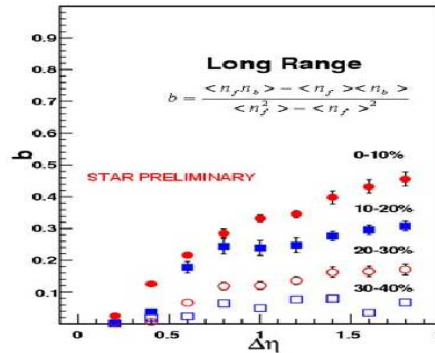


Fig. 14. Long range forward backward correlations in rapidity measured in the STAR experiment. Short range correlations have been subtracted.

The results on the forward backward rapidity correlations measured as a func-

tion of centrality has been reported by STAR<sup>47,48</sup> and PHOBOS<sup>49</sup> collaborations. The results shown in Figure 14 from the STAR experiment shows the correlation to be quite strong, with an increasing function of centrality of the collision. This could be qualitatively understood in terms of long range longitudinal fields, such as in the Glasma or string models<sup>50</sup>. An interesting analogy of the long range correlations could be made with the amplification of quantum fluctuations to macroscopic magnitudes in the early universe which form galaxies and clusters of galaxies<sup>50</sup>.

## 12. Disoriented chiral condensates

The QCD phase transition is predicted to be accompanied by chiral symmetry restoration at high temperatures and densities. One of the most interesting consequences of chiral transition is the formation of a chiral condensate in an extended domain, such that the direction of the condensate is misaligned from that of the true vacuum. This phenomenon is termed as the disoriented chiral condensates (DCC)<sup>51,52,53,54</sup>. The formation of DCC results in an excess of low momentum pions in a single direction in isospin space giving rise to large imbalances in the production of charged to neutral pions. This is studied in terms of the distribution of neutral pion fraction,  $f$ , given by,

$$f = \frac{N_{\pi^0}}{N_{\pi}}, \quad (12)$$

where  $N_{\pi^0}$  and  $N_{\pi}$  are the number of neutral pions and total pions, respectively. The pions in a normal event would follow a binomial form with a mean of 1/3, whereas within a domain of DCC the probability of pion fraction would follow a binomial distribution pattern such as,

$$P(f) = \frac{1}{2\sqrt{f}}.$$

The formation of DCC was hypothesized in the context of explaining observed abnormal events from cosmic ray experiments<sup>60,61</sup> which had either excess of charged-particles compared to neutrals (called Centauro events) or excess of neutrals with respect to charged-particles (anti-Centauro events). A dedicated experiment, MiniMax, was set up at the Tevatron at Fermilab to study  $p+\bar{p}$  collisions at  $\sqrt{s} = 1.8$  TeV<sup>62</sup>. At the SPS, both WA98 and NA49 experiments searched for the formation of DCC in heavy-ion collisions<sup>55,56,57,58,59</sup>.

A thorough DCC search in PbPb collisions at  $\sqrt{s_{NN}}=17.2$  GeV was performed by the WA98 Collaboration at CERN. This was based on a systematic study of photon and charged-particle multiplicity correlation using the data from a preshower photon multiplicity detector (PMD) and a silicon pad multiplicity detector (SPMD) for charged-particles. The analyses are performed using correlations of the number of photons to charged particles, wavelet techniques and power spectrum analysis of anomalous fluctuations in charged particles to photons. No clear DCC signal was observed and the upper limit for DCC production at 90% CL was established as a

16 *Tapan K. Nayak*

function of the fraction of DCC pions among all pions produced. An event display of the  $x - y$  positions of charged particle (SPMD) and photon (PMD) hits is shown in Figure 15 where a patch is marked which has a large number of photons to charged particles. A sliding window analysis<sup>63</sup> method has been employed to identify such events for proper characterization.

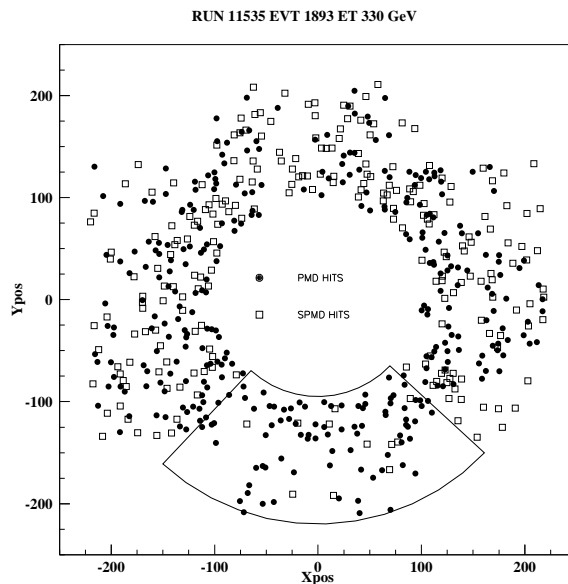


Fig. 15. Photon (PMD) and charged-particle (SPMD) hits in an azimuthal plane in the WA98 experimental set-up. The marked  $90^\circ$  patch corresponds to  $f_{\max}=0.77$ .

### 13. Fluctuations in the presence of jets

The presence of jets and minijets may affect the event-by-event fluctuation, which will be quite crucial at LHC energies. In order to make any inference about the fluctuation we need to understand the effect well. On the other hand, this study may help in our understanding of passage of jets through the medium. A study of fluctuations in  $p_T$  has been made in the presence of jets for simulated events at LHC energies<sup>26</sup>. The dependence of  $\Phi_{p_T}$  on a search window defined by,  $L_{\eta,\phi} = \sqrt{\Delta\eta^2 + \Delta\phi^2}$  has been studied for soft particles and soft+hard particles. The fluctuations seem to drastically increase in the presence of hard particles when the window in terms of  $L_{\eta,\phi}$  is increased. The expected jet production in Pb-Pb collisions at  $\sqrt{s_{NN}} = 5.5$  TeV for LHC energies would lead to large EbyE fluctuations of  $\langle p_T \rangle$ . This may allow one to test various models of jet production in the region not accessible by standard methods of jet detection. On the other hand,



fluctuations due to jet production should be taken into account when considering the fluctuations due to other processes.

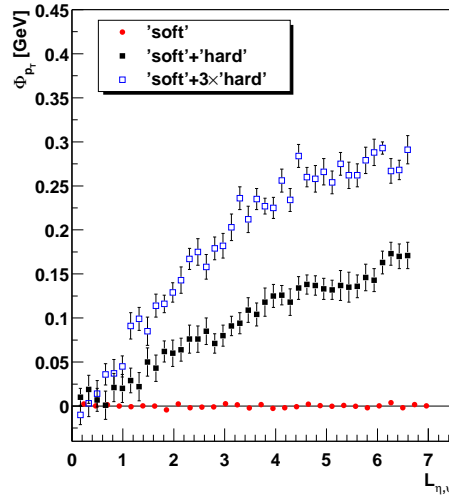


Fig. 16. The dependence of  $\Phi_{p_T}$  on the acceptance for 'soft' component (dots), 'hard' + 'soft' component (squares) and the contribution of hard component increased by a factor of 3 (open squares).

#### 14. Summary and outlook

Experiments at SPS and RHIC have given a wealth of data on fluctuations of various observables, some of the important ones have been discussed here. The extraction of dynamical fluctuations originating from QGP phase transition from the experimental results becomes complicated because of several competing processes. We have attempted to understand the importance of proper centrality selection for fluctuation studies in terms of a participant model. In order to infer any dynamical fluctuation arising from various physics processes one has to make sure that the fluctuations in number of participants are minimal. Available results have been discussed in terms of fluctuations in multiplicity, temperature and  $\langle p_T \rangle$ , elliptic flow, HBT radii, particle ratio, net charge and higher moments of net charge distributions, balance functions, long range correlations, formation of disoriented chiral condensates and presence of jets. Differential measures are being adopted in order to gain insight to the details of fluctuation. All these information have to be put together in order to arrive at the final conclusion.

One of the most important aspects of QGP study is the location of the critical point. It may be possible to access this experimentally by scanning the QCD

phase diagram in terms of baryon chemical potential and temperature. This can be accomplished by varying beam energies from about  $\sqrt{s_{\text{NN}}}=5$  GeV to 100 GeV. Such a program has recently been undertaken at RHIC<sup>64</sup>. Experiments at GSI<sup>65</sup> are planned to study this as well. At higher energies of LHC (Pb–Pb beams at  $\sqrt{s_{\text{NN}}}=5500$  GeV), the ALICE experiment will be able to make precise event-by-event measurements of various quantities and study their fluctuations<sup>26</sup>. With continued development in new analysis methods and theoretical advances, and with dedicated experiments, one will certainly learn a great deal more about QGP phase transition through fluctuation studies.

## References

1. S. Jeon and V. Koch, *Quark gluon plasma*, Edited by R.C. Hwa and X.N. Wang, (2003) 430, *Preprint* hep-ph/0304012.
2. H. Heiselberg, *Phys. Rep.* **351** (2001) 161.
3. T.K. Nayak, *Journal of Physics* **G32** (2006) S187-S194. *Preprint* nucl-ex/060802.
4. L. Van Hove, *Z. Phys.* **C27** (1985) 135.
5. M. A. Stephanov, K. Rajagopal and E. Shuryak, *Phys. Rev. Lett.* **81** (1998) 4816.
6. U. Heinz, *Preprint* nucl-th/0512051.
7. B. Mohanty, J. Alam, T.K. Nayak, *Phys. Rev.* **C67** (2003) 024904.
8. M.M. Aggarwal *et al.*, (WA98 Collaboration), *Phys. Rev.* **C65** (2002) 054912.
9. G. Baym and H. Heiselberg, *Phys. Lett.* **B469** (1999) 7.
10. K. Werner, *Phys. Rep.* **232** (1993) 87.
11. C. Alt *et al.*, (NA49 Collaboration), *Preprint* nucl-ex/0612010
12. S.S. Adler *et al.*, (PHENIX Collaboration), *Preprint* nucl-ex/0409015.
13. J. Mitchell *et al.* (PHENIX Collaboration), *Preprint* nucl-ex/0510076.
14. J. Adams *et al.* (STAR Collaboration), *Phys. Rev.* **C68** (2003) 044905.
15. R.L. Ray (STAR Collaboration) *Preprint* nucl-ex/0211030.
16. Hiroyuki Sato *et al.* (CERES Collaboration), *J. Phys.* **G30** (2004) S1371.
17. T. Anticic *et al.* (NA49 Collaboration), *Phys. Rev.* **C70** (2004) 034902
18. S.S. Adler *et al.* (PHENIX Collaboration), *Phys. Rev. Lett.* **93** (2004) 092301.
19. J. Adams *et al.* (STAR Collaboration) *Phys. Rev.* **C72** (2005) 044902.
20. J. Adams *et al.* (STAR Collaboration) *J. Phys.* **G32** (2006) L37.
21. S. Mrowczynski and E. Shuryak, *Acta Phys. Pol.* **B34** (2003) 4241.
22. R.S. Bhalerao and J-Y Ollitrault, *Physics Letters* **B641** (2006) 260.
23. P. Sorensen (STAR Collaboration), *Preprint* nucl-ex/0612021.
24. C. Loizides (PHOBOS Collaboration), *Preprint* nucl-ex/0701049.
25. O. Socolowski Jr. *et al.* *Phys. Rev. Lett.* **93** (2004) 182301.
26. Physics Performance Report, Volume II, ALICE Collaboration, *Journal of Physics* **G32** (2006) 1295.
27. C. Roland, *J. Phys.* **G30** (2004) S1381.
28. S. Das *et al.* (STAR Collaboration), *Preprint* nucl-ex/0503023.
29. G. Torrieri, S. Jeon and J. Rafelski, *Preprint* nucl-th/0510024
30. Georgio Torrieri, *Eur. Phys. Journal* **C49** (2007) 287. *Preprint* nucl-th/0702020
31. M. Asakawa, U. Heinz, B.Muller, *Phys. Rev. Lett.* **85** (2000) 2072.
32. S. Jeon and V. Koch, *Phys. Rev. Lett.* **85** (2000) 2076.
33. E. Shuryak and M.A. Stephanov, *Phys. Rev.* **C63** (2001) 064903.
34. C. Alt *et al.* (NA49 Collaboration), *Phys. Rev. C* **70** (2004) 064903.
35. K. Adcox *et al.* (PHENIX Collaboration), *Phys. Rev. Lett.* **89** (2002) 082301.

36. C. Pruneau, S. Gavin, S. Voloshin, Phys. Rev. **C66** (2002) 044904.
37. J.T. Mitchell, J. Phys **G30** (2004) S819.
38. S. Ejiri, F. Karsch and K. Redlich, Phys. Lett. B633 (2006) 275.
39. R. V. Gavai and S. Gupta, Phys. Rev. **D72** (2005) 054006.
40. K. Redlich, B. Friman and C. Sasaki, *Preprint* nucl-ex/0702296.
41. S. A. Bass, P. Danielewicz and S. Pratt, Phys. Rev. Lett. **85** (2000) 2689.
42. P. Bozek, Phys. Lett. **B609** (2005) 247.
43. J. Adams *et al.*, (STAR Collaboration) Phys. Rev. Lett. **90** (2003) 172301.
44. C. Alt *et al.* (NA49 Collaboration), Phys. Rev. **C71** (2005) 034903;
45. P. Christakoglou *et al.* (NA49 Collaboration), *Preprint* nucl-ex/0510045.
46. A. Capella *et al.* Phys. Rep. **236** (1994) 225.
47. Terence Tarnowsky *et al.* (STAR Collaboration), *Preprint* nucl-ex/0606018
48. Brijesh Srivastava *et al.* (STAR Collaboration), *Preprint* nucl-ex/0702042.
49. B.B. Back *et al.* (PHOBOS Collaboration) Phys. Rev. **C74** (2006) 011901.
50. Larry McLerran *Preprint* nucl-ex/0702004.
51. J.-P. Blaizot and A. Krzywcki, Phys. Rev. **D46** (1992) 246.
52. J.D. Bjorken, K.L. Kowalski and C.C. Taylor, SLAC-PUB-6109, April 1993.
53. K. Rajagopal, F. Wilczek, Nucl. Phys. **B399** (1993) 399.
54. Bedanga Mohanty, Julien Serreau, Phys. Rep. **414** (2005) 263.
55. M. M. Aggerwal *et al.* (WA98 Collaboration), Phys. Lett. **B420** (1998) 169.
56. M. M. Aggerwal *et al.* (WA98 Collaboration), Phys. Rev. **C64** (2001) 011901.
57. M. M. Aggerwal *et al.* (WA98 Collaboration), Phys. Rev. **C67** (2003) 044901.
58. H. Appelshauser *et al.* (NA49 Collaboration), Phys. Lett. **B459** (1999) 679.
59. T.K. Nayak *et al.* (WA98 Collaboration), Nucl. Phys. **A638** (1998) 249c.
60. C.M.G. Lates, Y. Fujimoto and S. Hasegawa, Phys. Rep. **65** (1980) 151
61. E.Gładysz-Dziaduś, INP Report No.1879/PH, Cracow, 2001.
62. T.C. Brooks *et al.*, Phys. Rev. **D55** (1997) 5667.
63. M.M.Aggarwal *et al.* (WA98 Collaboration), Pramana **60** (2003) 987.
64. T. Ludlum *et al.* BNL-75692-2006, Proceedings of the workshop on “Can we discover the QCD Critical point at RHIC?”, March 9-10, 2006.
65. C. Hohne *et al.* (CBM Collaboration) Nucl. Phys. **A749** (2005) 141.